possibility involving no hydride permutation gave a slightly better fit to the data and was, therefore, marginally preferred.

The physical mechanisms that correspond to the experimentally established permutations considered were examined by employing a quasi-least-motion simulation. We have concluded that the most probable mechanism involves a simultaneous exchange of the two axial phosphorus ligands with two of the equatorial phosphorus ligands. The hydride ligands simply move to the new equatorial edges. In the (distorted) distal pentagonal-bipyramidal structure that is favored as the equilibrium geometry, this corresponds to permutation of the CrP_5 framework via a "Berry pseudorotation" type process.

Line-shape analysis in a seven-spin system is a complex problem; the NMR line-shape study of $CrH_2[P(OCH_3)_3]_5$ described in this paper involves an analysis of the most complex spin system yet treated in detail and further illustrates the power of a systematic analysis of the basic permutations to clarify and eliminate mechanistic possibilities.

Acknowledgment. We wish to acknowledge the fine technical assistance of M. A. Cushing, Jr., G. Watunya, and F. N. Schock.

Appendix

In order to facilitate the visualization of dynamical processes such as mutual exchange in coordination complexes, electrocyclic reactions, and intramolecular Diels–Alder reactions, we have developed a methodology for mapping an initial atomic configuration into a final one. The first step is to assure maximum coincidence of the (labeled) atoms in the initial and final arrangements. This is accomplished by requiring that the mass-weighted residual be at a minimum

$$m^i[R^i(\text{final}) - R^i(\text{initial})]^2$$

where the R^i's are particle position vectors. It is generally convenient to operate in a center-of-mass coordinate system, though with simple coordination complexes it may be acceptable to place the origin at the central atom. The second step involves motion along some pathway leading from the initial to the final configuration. Least-motion pathways defined in Cartesian coordinates are generally unsuitable, giving physically unreasonable intermediate structures. *Quasi-least-motion* pathways may be mapped, either in spherical polar coordinates (suitable for simple coordination complexes) or in internal coordinates (the most general case). While these pathways will not in general correspond to the lowest energy route from starting material to products, they should represent qualitative approximations of the actual pathways.

We have used the spherical polar model for the rearrangement mechanisms for the distal isomer of $CrH_2[P(OCH_3)_3]_5$. The trimethyl phosphite ligands were replaced by points of equal mass displaced outward along the Cr–P bond direction to the center-of-mass for the phosphite group.

Registry No. $Cr[P(OMe)_3]_5H_2$, 92842-95-0; $Cr[P(OMe)_3]_6$, 70948-62-8.

Trinuclear Clusters of Early Transition Metals: Jahn–Teller Distortions and Electronic Structure†

Yuansheng Jiang* (Yuan-sun Kiang) and Aoqing Tang

Institute of Theoretical Chemistry, Jilin University, Changchun, Peoples Republic of China

Roald Hoffmann*

Department of Chemistry, Cornell University, Ithaca, New York 14853

Jinling Huang* and Jiaxi Lu

Fujian Institute of Research on the Structure of Matter, Academia Sinica, Fuzhou, Peoples Republic of China

Received April 18, 1984

A detailed theoretical study of a trinuclear eight-electron cluster with a distorted metal core, $Mo_3S_2Cl_9^{3-}$, leads to some general conclusions about the role of different capping, bridging, and terminal ligands in determining the electronic and geometrical structure of trinuclear clusters of the early transition metals.

The early transition-metal cluster compounds are distinguished from similar clusters involving 8B elements by the typically high oxidation state of the metal component and by halogens or other electronegative atoms as ligands. A variety of oxidation states or electron counts exists. During the past few years, much research has been carried out on and much attention has been paid to the trinuclear metal cluster systems, one of the representative species of experimental and theoretical importance.[1] Dozens of complexes of this type have been prepared and structurally characterized.[2-43] At the same time, theoretical investigations were also developing.[44-49]

†Dedicated to the memory of our friend and colleague Earl Muetterties.

(1) Müller, A.; Jostes, R.; Cotton, F. A. *Angew. Chem., Int. Ed. Engl.* **1980**, *19*, 875.
(2) Cotton, F. A.; Mague, J. T. *Inorg. Chem.* **1965**, *3*, 1402.
(3) Goldberg, S. Z.; Spinack, B.; Stanley, G.; Eisenberg, R.; Braitsch, D. M.; Muller, J. S.; Abkowitz, M. *J. Am. Chem. Soc.* **1977**, *99*, 110.
(4) King, R. B.; Braitsch, D. M.; Kapoor, P. N. *J. Am. Chem. Soc.* **1975**, *97*, 60.
(5) Fisher, E. O.; Rohrscheid, F. *J. Organomet. Chem.* **1966**, *6*, 53.
(6) Churchill, M. R.; Chang, S. W. Y. *J. Chem. Soc., Chem. Commun.* **1974**, 248.
(7) Müller, A.; Ruck, A.; Dartmann, M.; Reinsch-Vogell, U. *Angew. Chem., Int. Ed. Engl.* **1981**, *20*, 483.

0276-7333/85/2304-0027$01.50/0 © 1985 American Chemical Society

Table I. Some Trinuclear Clusters and Their Selected Properties

compound	type	electron count	M-M, Å	ref
Re_3Cl_9	U_3	12	2.489	2
$[Nb_3Cl_6(C_6Me_6)_3]^{2+}$	U_6	7		3
$[Ta_3Cl_6(C_6Me_6)_3]^{+}$	U_6	8		4, 5
$[Nb_3Cl_6(C_6Me_6)_3]^{+}$	U_6	8	3.334	4-6
$[Nb_3Br_6(C_6Me_6)_3]^{+}$	U_6	8	3.335	4, 5
$[Mo_3O_4F_9]^{5-}$	M_3	6	2.502	7
$[Mo_3S_4Cp_3]^{+}$	M_3	6	2.812	8
$[Mo_3S_4(CN)_9]^{5-}$	M_3	6	2.766	9
$[Mo_3O_4(C_2O_4)_3(H_2O)_3]^{2-}$	M_3	6	2.486	10
$Mo_3O_4(acac)_3(EtO)_3$	M_3	6	2.47	11
$[Mo_3S_{13}]^{2-}$	M_3	6	2.77	12
$[W_3O_4F_4]^{5-}$	M_3	6	2.514	13
$W_3O_3Cl_5(Oac)(PBu_3)_3$	M_3	6	2.609	14
$[Mo_3O_2S(Hnta)_3]^{2-}$	M_3	6	2.589	15
$[Mo_3S_4(SCH_2CH_2S)_3]^{2-}$	M_3	6	2.78	16
$Zn_2Mo_3O_8$	M_3	6	2.524	17
$LiZn_2Mo_3O_8$	M_3	7	2.578	18
$Mo_3S_4Cp_3$	M_3	7		19
Nb_3Cl_8	M_3	7	2.81	20
Nb_3Br_8	M_3	7	2.88	21
Nb_3I_8	M_3	7	3.00	21
$[Mo_3OCl_3(Oac)_3(H_2O)_3]^{2+}$	M_3	8	2.550	22
$[Mo_3OCl_3(Oac)_3Cl_3]^{-}$	M_3	8	2.579, 2.585, 2.567	23
$Zn_3Mo_3O_8$	M_3	8	2.58	18
$[V_3O(Oac)_6(CH_3COOH)_2(THF)]^{+}$	M_6	6	3.307	24
$V_3O(CF_3CO_2)_6(THF)_3$	M_6	7	3.357	24
$[W_3O(Oac)_6(H_2O)_3]^{2+}$	M_6	8	2.701, 2.715	25
$[Cr_3O(Oac)_6(H_2O)_3]^{+}$	M_6	9	3.274	26
$Cr_3O(CHF_2CO_2)_6(4\text{-}CNC_5H_4)_3$	M_6	10	3.336	27
$Cr_3O(CHF_2CO_2)_6(C_5H_5N)_3$	M_6	10	3.356	27
$Mn_3O(Oac)_6(HOAc)(Oac)_{2/2}$	M_6	12	3.27	28
$Mn_3O(Oac)_6(C_5H_5N)_3$	M_6	13		29
$Mn_3O(Oac)_6(3\text{-}ClC_5H_4N)_3$	M_6	13	3.363	30
$[Fe_3O(Oac)_6(H_2O)_3]^{+}$	M_6	15	3.29	31
$[Mo_3S_2Cl_9]^{3-}$	B_3	8	2.556, 2.641, 2.653	32
$[Nb_3O_2(Me_3CCO_2)_6(C_4H_8O)_3]^{+}$	B_6	4	2.842	33
$Mo_3O(OR)_{10}$	B_6	4	2.53	34
$[Nb_3O_2(SO_4)_6(H_2O)_3]^{5-}$	B_6	4	2.875, 2.892	35
$[Mo_3(CCH_3)_2(Oac)_6(H_2O)_3]^{2+}$	B_6	4	2.883-2.891	36
$[Mo_3(CCH_3)_2(Oac)_6(H_2O)_3]^{+}$	B_6	5	2.815, 2.807, 2.820	36
$[Mo_3O_2(Oac)_6(H_2O)_3]^{2+}$	B_6	6	2.766	37, 38
$[Mo_3O_2(O_2CEt)_6(H_2O)_3]^{2+}$	B_6	6	2.752	37
$Mo_3O_2(Oac)_6(H_2O)(OH)_2$	B_6	6	2.796, 2.773	39
$[Mo_3O(CCH_3)(Oac)_6(H_2O)_3]^{+}$	B_6	6	2.752	40
$[W_3O_2(Oac)_6(H_2O)_3]^{2+}$	B_6	6	2.747	41, 42
$[W_3O_2(O_2CEt)_6(H_2O)_3]^{2+}$	B_6	6	2.745	41, 42
$[W_3O_2(Oac)_6(Oac)_3]^{-}$	B_6	6	2.769	41
$W_3O_2(O_2CCMe_3)_6(O_2CCMe_3)_2(H_2O)$	B_6	6	2.76	41
$[Mo_3O_2(Oac)_6(OCH_3)_3]^{-}$	B_6	6	2.76, 2.81	43

Müller, Jostes, and Cotton[1] have reviewed in a systematic way the main achievements in this field prior to 1980. They classified these compounds into three categories according to the number of capping ligands (μ_3-type) in-

(8) Vergarmini, P. J.; Vahrenkamp, H.; Dahl, L. F. *J. Am. Chem. Soc.* **1971**, *93*, 6327.
(9) Müller, A.; Reinsch, U. *Angew. Chem., Int. Ed. Engl.* **1980**, *19*, 72.
(10) Bino, A.; Cotton, F. A.; Dori, Z. *J. Am. Chem. Soc.* **1978**, *100*, 5252; **1979**, *101*, 8842.
(11) Scanicar, S.; Herceg, M. *Acta Crystallogr.* **1966**, *21*, A151.
(12) Müller, A.; Pohl, S.; Dartmann, M.; Cohen, J. P.; Bennett, J. M.; Kirchner, R. M. *Z. Naturforsch., B: Anorg. Chem., Org. Chem.* **1979**, *B34*, 434.
(13) Mattes, R.; Mennemann, K. *Z. Anorg. Allg. Chem.* **1977**, *437*, 175.
(14) Sharp, P. R.; Schrock, R. R. *J. Am. Chem. Soc.* **1980**, *102*, 1430. Cotton, F. A.; Felthouse, T. R.; Lay, D. G. *J. Am. Chem. Soc.* **1980**, *102*, 1431.
(15) Shibahara, T.; Hattori, M.; Kuroya, M. *J. Am. Chem. Soc.* **1984**, *106*, 2710.
(16) Halbert, T. R.; McGavley, K.; Pan, W.-H.; Czernuszewicz, R. S.; Stiefel, E. I. *J. Am. Chem. Soc.* **1984**, *106*, 1849.
(17) (a) McCarroll, W. H.; Katz, L.; Ward, R. *J. Am. Chem. Soc.* **1951**, *79*, 5410. (b) Ansell, G. B.; Katz, L. *Acta Crystallogr.* **1966**, *21*, 482.
(18) Torardi, C. C.; McCarley, R. E. *Inorg. Chem.* **1984**, *23*, 0000.
(19) Beck, W.; Danzer, W.; Thiel, G. *Angew. Chem., Int. Ed. Engl.* **1973**, *12*, 582.
(20) Schnering, H.-G.; Wöhrle, H.; Schäfer, H. cited in: Schäfer, H.; Schnering, H.-G. *Angew. Chem.* **1969**, *76*, 833.
(21) Simon, A.; Schnering, H.-G. von *J. Less-Common Met.* **1966**, *11*, 31.
(22) Bino, A.; Cotton, F. A.; Dori, Z. *Inorg. Chim. Acta* **1979**, *33*, L133.
(23) Huang, J.; Shang, M.; Huang, J.; Zhang, H.; Lu, S.; Lu, J. *J. Struct. Chem. (Engl. Transl.)* **1982**, *1*, 1.
(24) Cotton, F. A.; Lewis, G. E.; Mott, G. N. *Inorg. Chem.* **1982**, *21*, 3316.
(25) Ardon, M.; Cotton, F. A.; Dori, Z.; Fang, A.; Kapon, M.; Reisner, G. M.; Shaia, M. *J. Am. Chem. Soc.* **1982**, *104*, 5394.
(26) Chang, S. C.; Jeffrey, G. A. *Acta Crystallogr., Sect. B.* **1970**, *B26*, 673.
(27) Cotton, F. A.; Wang, W. *Inorg. Chem.* **1982**, *21*, 2675.
(28) Hessel, L. W.; Romers, C. *Recl. Trav. Chim. Pays-Bas* **1669**, *88*, 545.
(29) Baikie, A. R. E.; Hursthouse, M. B.; New, D. B.; Thornton, P. *J. Chem. Soc., Chem. Commun.*, **1978**, 62.
(30) Baikie, A. R. E.; Hursthouse, M. B.; New, D. B.; Thornton, P.; White, R. G. *J. Chem. Soc., Chem. Commun.*, **1980**, 684.
(31) Anzenhofer, K.; de Boer, J. J. *Recl. Trav. Chim. Pays-Bas* **1969**, *88*, 286.

Scheme I

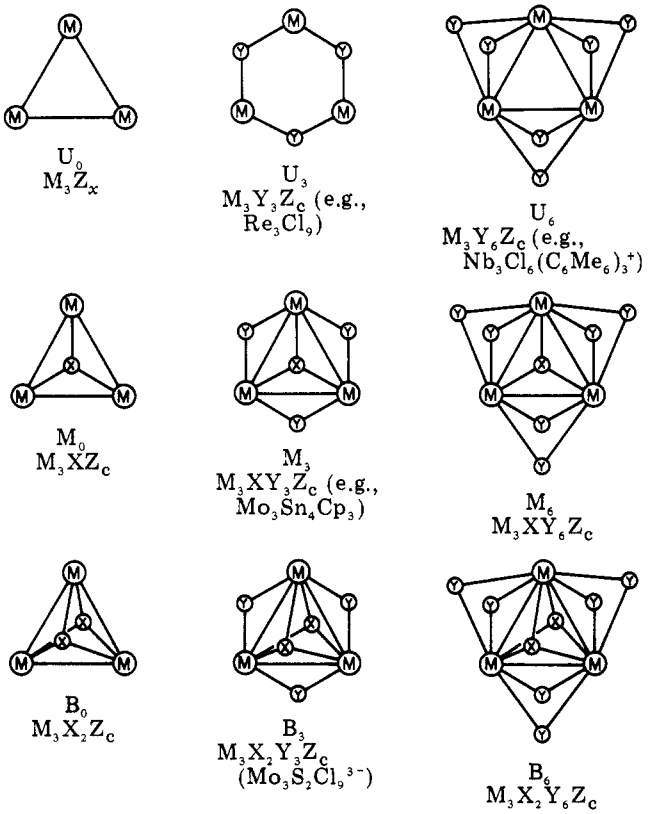

volved and designated them by capital letters A, B, and C, corresponding to zero, one, or two μ_3-ligands contained, respectively. For the purpose of the present investigation, it seems instructive to classify them in terms of the number of capping and bridging atoms simultaneously. We will use symbols M, B, and U to describe the number of capping or μ_3 ligands (M = mono-, B = bi-, and U = uncapped) and a subscript (0, 3, 6) to count the number of bridging or μ_2 atoms. The μ_3 or capping ligand will be called generally X, the μ_2 ligand Y, and the terminal ligands Z. Some typical examples are shown in Scheme I, where no attention is paid to drawing out the stereochemistry of the μ_2 ligands in detail, nor are the μ_1 or terminal ligands drawn in. We have tentatively skirted the nontrivial issue of whether a bidentate polyatomic ligand that bridges two metals, e.g., acetate or sulfate, is really μ_2 or two μ_1 ligands (1). For the moment we count it as the equivalent of two

1

terminal ligands but, as our subsequent calculations will show, the detailed nature of the bidentate ligand cannot be ignored. Also note that this MXYZ nomenclature puts the terminal Z ligands in a subsidiary role. This is something we will discuss in some detail later. It is not a simple matter, for some μ_1 ligands in these systems are labile, weakly bound, but in other cases (e.g., terminal oxo groups) very strongly held. Finally, we will give primacy to electronic considerations rather than simple ligand or atom counting in deciding where a ligand fits in. Thus a terminal arene or cyclopentadienyl will be classified as Z_3. Table I lists some of the compounds known.

It can be seen from Table I that most of these compounds have electron counts from 6 to 8 with respect to the metal core except Re_3Cl_9, a U_3 compound, and those M_6 compounds with electron counts ranging from 7 to 13 and characterized by unusually long M–M distances. The effective symmetries of the cluster cores are either D_{3h} or C_{3v}, with a few exceptions showing tiny distortion. However, one novel compound of the M_3-type, whose molecular formula is $[Mo_3S_2Cl_9]^{3-}$, with eight electrons in the metal core, interestingly exhibits unequal M–M bond distances relative to its idealized D_{3h} symmetry.[32] The structural details of this molecule are shown in **2** and the Appendix.

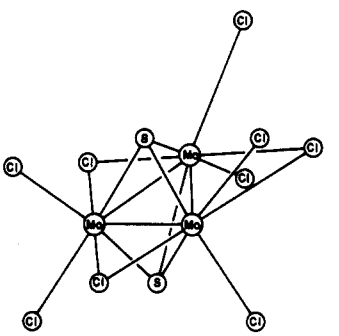

2

Of the three Mo–Mo bonds, two are approximately equal but longer than the third, with the maximum difference equal to 0.097 Å. Similarly, a couple of the Mo–S bonds located between the two longer Mo–Mo bonds are shorter than the remaining four. Their maximum difference is 0.11 Å. The molecule also contains two kinds of Mo–Cl bonds, one involving μ-Cl and the other involving terminal chlorine atoms, which also show unequal lengths with smaller differences of 0.025 and 0.045 Å, respectively. Such a significant distortion in the cluster skeleton must have electronic origins and formed the initial stimulus to this study.

We have carried out extended Hückel calculations of the electronic structure of $Mo_3S_2Cl_9^{3-}$, in order to gain a better

(32) Huang, J.; Shang, M.; Lui, S.; Lu, J. *Sci. Sin. (Engl. Transl.)* **1982**, *25*, 1270.
(33) Cotton, F. A.; Duraj, S. A.; Roth, W. J. *J. Am. Chem. Soc.* **1984**, *106*, 3527.
(34) R = CH_2-*t*-Bu, *i*-Pr: Chisholm, M. H.; Folting, K.; Huffman, J. C.; Kirkpatrick, C. C. *Inorg Chem.* **1984**, *23*, 1021.
(35) Bino, A. *Inorg. Chem.* **1982**, *21*, 1917.
(36) Ardon, M.; Bino, A.; Cotton, F. A.; Dori, Z.; Kapon, M.; Kolthammer, B. W. S. *Inorg. Chem.* **1981**, *20*, 4082.
(37) Ardon, M.; Bino, A.; Cotton, F. A.; Dori, Z.; Kaftory, M.; Reisner, G. *Inorg. Chem.* **1982**, *21*, 1912.
(38) Cotton, F. A.; Dori, Z.; Marler, D. O.; Schwotzer, W. *Inorg. Chem.* **1983**, *22*, 3104.
(39) Birnbaum, A.; Cotton, F. A.; Dori, Z.; Marler, D. O.; Reisner, G. M.; Schwotzer, W.; Shaia, M. *Inorg. Chem.* **1983**, *22*, 2723.
(40) (a) Bino, A.; Cotton, F. A.; Dori, Z. *J. Am. Chem. Soc.* **1981**, *103*, 243. (b) Bino, A.; Cotton, F. A.; Dori, Z.; Kolthammer, B. W. S. *J. Am. Chem. Soc.* **1981**, *103*, 5779. (c) Bino, A.; Cotton, F. A.; Dori, Z.; Falvello, L. R.; Reisner, G. M. *Inorg. Chem.* **1982**, *21*, 2750.
(41) Bino, A.; Cotton, F. A.; Dori, Z.; Koch, S.; Küppers, H.; Millar, M.; Sekutowski, J. C. *Inorg. Chem.* **1978**, *17*, 3245.
(42) Bino, A.; Hesse, K. F.; Küppers, H. *Acta Crystallogr., Sect. B* **1980**, *B36*, 723.
(43) Birnbaum, A.; Cotton, F. A.; Dori, Z.; Kapon, M. *Inorg. Chem.* **1984**, *23*, 1617.
(44) Cotton, F. A.; Haas, T. E. *Inorg. Chem.* **1964**, *3*, 10.
(45) Cotton, F. A. *Inorg. Chem.* **1964**, *3*, 1217.
(46) Bursten, B. E.; Cotton, F. A.; Stanley, G. G. *Isr. J. Chem.* **1980**, *19*, 132.
(47) Bursten, B. E.; Cotton, F. A.; Hall, M. B.; Najjar, R. C. *Inorg. Chem.* **1982**, *21*, 302.
(48) Chisholm, M. H.; Cotton, F. A.; Fang, A.; Kober, E. M. *Inorg. Chem.* **1984**, *23*, 749.
(49) Fang, A. Ph.D. Dissertation, Texas A&M University, 1982.

Table II. Symmetry-Adapted Linear Combinations for Mo_3

atomic orbitals	molecular orbitals
z^2	$a'_1 + e'$
xz	$a''_2 + e'$
yz	$a''_2 + e''$
xy	$a''_1 + e''$
$x^2 - y^2$	$a'_1 + e'$

understanding of the causes of the distortion existing in this anion. Interactions between the metal core and various ligand fragments are compared by displaying a series of correlation diagrams that present a qualitative picture of the role that each kind of ligand is playing as well as their couplings. General relationships between geometry and electron count are analyzed in terms of energy level sequences. These lead to an understanding of the geometrical trends not only of the eight-electron B_3 cluster $Mo_3S_2Cl_9^{3-}$ but also of the other molecules displayed in Table I. In particular we will find a significant role for a Jahn–Teller distortion for certain specific electron counts.

The Electronic Structure of $Mo_3S_2Cl_9^{3-}$

We began with a calculation on this trinuclear cluster in idealized D_{3h} symmetry, the bond lengths and angles averaged from the experimental structure. The geometrical details and particulars of the extended Hückel calculations are given in the Appendix. With the normal oxidation state assignments of 1– for Cl and 2– for S one obtains a deficit of 10 electrons for the Mo_3 core or a total of 8 electrons distributed over the three metals.

Though this is not the way the computer program operates, it is convenient to work in a coordinate system adapted to local symmetry, i.e. one with radial (z), tangential (x), and perpendicular (y) orbitals, as shown in 3,

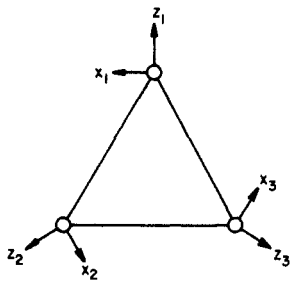

3

where all the y axes are parallel to one another and perpendicular to the triangle plane, the z axes intersect at and point away from the center of the triangle, and the tangential x axes are fixed by requiring a right-handed coordinate system. If χ_1, χ_2, and χ_3 represent an equivalent atomic orbital set defined with respect to each of the three Mo atoms, then the following transformation will construct symmetry orbitals of species a and e, namely

$$\begin{vmatrix} \psi_a \\ \psi_{e_a} \\ \psi_{e_b} \end{vmatrix} = \begin{vmatrix} \frac{1}{\sqrt{3}} & \frac{1}{\sqrt{3}} & \frac{1}{\sqrt{3}} \\ \frac{2}{\sqrt{6}} & -\frac{1}{\sqrt{6}} & -\frac{1}{\sqrt{6}} \\ 0 & \frac{1}{\sqrt{2}} & -\frac{1}{\sqrt{2}} \end{vmatrix} \begin{vmatrix} \chi_1 \\ \chi_2 \\ \chi_3 \end{vmatrix}$$

where a denotes one of the four species a'_1, a'_2, a''_1, and a''_2 and e represents e′ or e″. The five 3d orbitals at each center will combine in the way indicated in Table II.

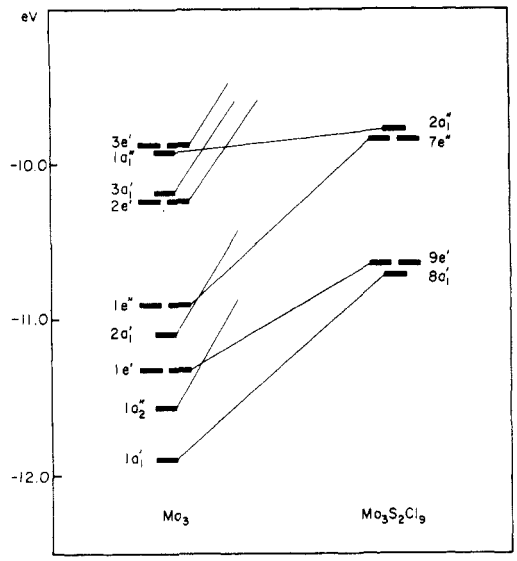

Figure 1. Lower d block levels of the Mo_3 core and the related frontier levels in the $[Mo_3S_2Cl_9]$ cluster.

Within each orbital set the topology of the interactions then sets the level ordering. In some cases the nondegenerate a type orbital is at low energy, in some cases the degenerate e orbitals. It is easy to decide which pattern it should be. For instance 4–8 show the nondegenerate combinations. These are clearly bonding for z^2, yz, and $x^2 - y^2$ but antibonding for xy and xz.

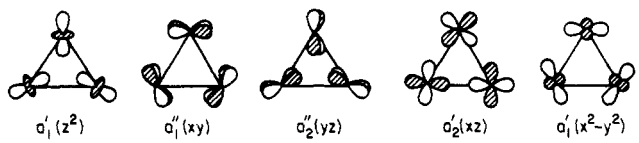

4 **5** **6** **7** **8**

In Figure 1 we show the lower levels of the Mo_3 core and the $Mo_3S_2Cl_9$ cluster. The ten lowest levels of the Mo_3 cluster core are exactly as anticipated, the bonding combinations $a'_1(z^2) + a''_2(yz) + e'(xz) + a'_1(x^2 - y^2) + e''(xy)$. Not all of these survive the perturbation impressed by the S and Cl ligands in $Mo_3S_2Cl_9^{3-}$. The geometry of the incoming donors clearly destabilizes all the d block levels (except $1a''_1$ which has too many nodes to interact with any S or Cl σ-bonding combination). However $1a''_2$ and $2a'_1$, which "point" toward the sulfurs and chlorines, are clearly affected most, pushed up and out of the frontier region.

Note the nice closed-shell configuration for a six-electron count ($8a'_1 + 9e'$ filled). One is perfectly well justified in characterizing the six-electron system as possessing three metal–metal σ bonds, for the set of three such localized bonds would transform as $a'_1 + e'$. The composition of the $a'_1 + e'$ set is also consistent with a set of three σ bonds.

For an eight-electron count, two electrons enter the degenerate $7e''$ orbital. One would expect either a symmetrical (D_{3h}) ground-state triplet or a distorted low-spin state. We will return to a general discussion of the M_3 clusters and the effect of substituents on the level ordering, but before we do that we wish to discuss the potential deformation of the eight-electron system in some detail.

The Jahn–Teller Distortion in $Mo_3S_2Cl_9^{3-}$

Given two electrons in an e orbital of a threefold symmetric system, the Jahn–Teller theorem[50,51] tells us that

(50) Jahn, H. A.; Teller, E. *Proc. R. Soc. London, Ser. A* **1937**, *161*, 220.
(51) Longuet-Higgins, H. C.; Öpik, U.; Pryce, M. H. L.; Sack, R. A. *Proc. R. Soc. London, Ser. A* **1958**, *244*, 1.

Table III. Computed Energy Minima for $[Mo_3S_2Cl_9]^{3-}$

	minimum 1	minimum 2
Mo-Mo, Å	2.637, 2.578	2.583, 2.680
Mo-S, Å	2.407, 2.313	2.347, 2.435
α, deg	117	125
β, deg	3	−3
stabilization,[a] eV	0.115	0.138
HOMO stabilization, eV	0.105	0.133

[a] Relative to D_{3h} form: $\alpha = 120°$ and $\beta = 0°$.

a vibrational mode of e symmetry exists that will remove this symmetry. One such mode is E′, shown in **9**.[52] The

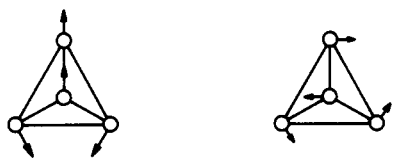

9

E′$_a$ component maintains C_{2v} symmetry, which is convenient. Let us assume that the Cl atoms remain fixed and only the Mo and S atoms move. This assumption is based on a fragment calculation which shows that the partly filled HOMO (e″) is 95% on the Mo_3S_2 core.

The molybdenum motion may be measured by the angle α spanned by the lines connecting the center of the triangle and the two bottom Mo atoms, as in **10**. The sulfur

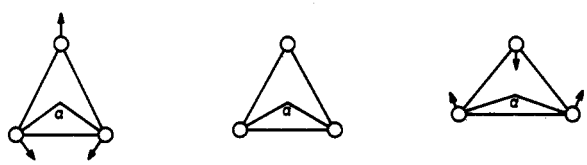

10

motion can be followed by an angle β between the lines connecting the center of the molecule to the initial and final positions of a moving capped atom. If $\beta > 0$, the S atoms move toward the upper Mo, and if $\beta < 0$, the S atoms move toward the midpoint of the bottom Mo–Mo line. The combined motions are shown in **11**.

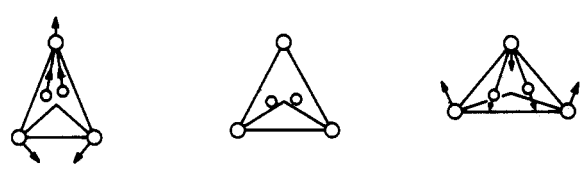

11

(52) Herzberg, G. (1) "Infrared and Raman of Polyatomic Molecules"; Van Nortrand: Princeton, NJ, 1945. (2) "Molecular Spectra and Molecular Structure"; Van Nortrand-Rinhold: New York, 1966; Vol. III.

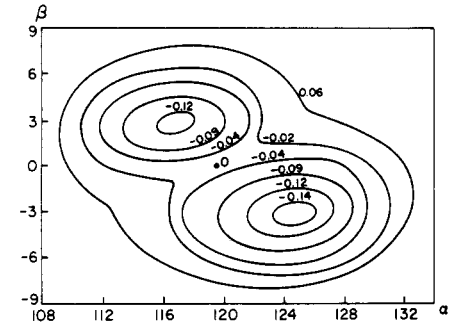

Figure 2. Energy surface of the Jahn–Teller distortion, with respect to the variation of α and β.

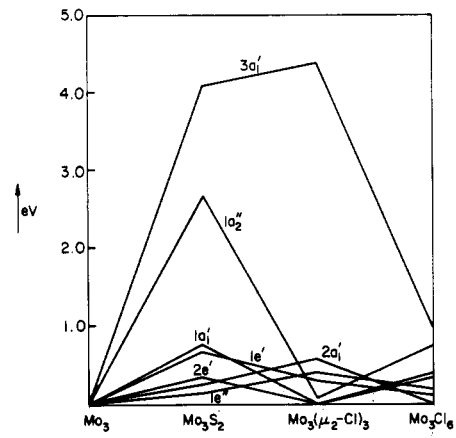

Figure 3. Destabilization of the lower d block levels relative to the unperturbed Mo_3 core.

A potential energy surface is calculated varying α and β. This is presented in Figure 2. There is a double minimum, as expected, for the combined α and β variation. The computed minima occur with the geometrical parameters specified in Table III. Minimum 1 agrees well with the dimensions of the observed structure, which has Mo–Mo distances of 2.647 and 2.556 Å and Mo–S distances of 2.399 and 2.326 Å. The energy of stabilization of the molecule and the HOMO (e″) are listed also in Table III. It is clear that the partly filled e″ HOMO is the prime contributor to the stabilization of the molecule.

Influence of the Ligands

Let us now return to the symmetrical $Mo_3S_2Cl_9$ system and see if we can glean the relative importance of the interactions with the different types of ligands present—the μ_3-S, the μ-Cl, and the terminal Cl. We carry out a calculation on $Mo_3(\mu_3\text{-}S)_2$, $Mo_3(\mu\text{-}Cl)_3$, and Mo_3Cl_6, i.e., the Mo_3 core plus each type of ligand separately. The Mo_3 d orbitals are destabilized by any interaction with additional ligands, the extent of such destabilization being a rough measure of the stabilizing interaction that must occur in low-lying bonding levels. This is essentially an angular overlap model argument. Figure 3 collects these destabilizations for the lower d block levels, all relative to the unperturbed Mo_3 core.

One would not expect the destabilizations to be entirely uniform for each pattern of substitution (capping vs. bridging vs. terminal) carries its own symmetry constraints. Nevertheless, a general ordering does obtain: $(\mu_3\text{-}S)_2 > (\mu\text{-}Cl)_3 > (Cl)_6$; i.e., the capping ligands play the leading role and the terminal ligands influence the d block least.

Next let us apply the perturbations of these ligands in sequence. Figure 4 shows the energy levels of Mo_3, $Mo_3(\mu_3\text{-}S)_2$, $Mo_3(\mu_3\text{-}S)_2(\mu\text{-}Cl)_3$, and the complete $Mo_3S_2Cl_9$ complex. The sequence is instructive because it shows that

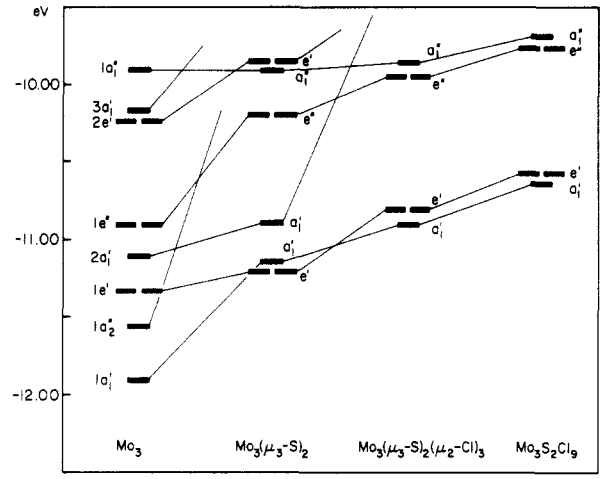

Figure 4. Correlation of d block levels of Mo_3, $Mo_3(\mu_3\text{-}S)_2$, $Mo_3(\mu_3\text{-}S)_2(\mu\text{-}Cl)_3$, and $Mo_3(\mu_3\text{-}S)_2(\mu\text{-}Cl)_3Cl_6$.

while the capping S ligands are energetically most important, they are not sufficient to set the final level order. The $2a'_1$ orbital of the Mo_3 cluster needs the ligand field of the bridging halides to be destabilized. The terminal ligands are not important to the level sequence, as the last stage of substitution shows. In this case, the good closed-shell electron counts for the metal core should be 6, 8, or 12. This is in agreement with the known U_3-type compound Re_3Cl_9.

It is clear that both the capping and bridging ligands are important in setting the level sequence. The caps destabilize $1a''_2$ of the Mo_3 cluster, the bridges $2a'_1$. In a general $M_3(\mu_3\text{-}A)_2(\mu\text{-}B)_3C_6$ cluster if A or B are weak σ donors, then a different level sequence could result, with either $1a''_2$ or $2a'_1$ below the e'' MO which is responsible for the Jahn–Teller distortion of the eight-electron cluster. Such eight-electron systems would not half-fill a degenerate level and so should maintain threefold symmetry.

We note here that there is evidence for seven- and eight-electron bicapped clusters in the electrochemistry of the $Mo_3O(OR)_{10}$ clusters of Chisholm and co-workers.[48] These authors have also presented molecular orbital calculations for their clusters that also indicate an e'' level filled by the seventh and eighth electrons, and they recognize clearly the possibility of Jahn–Teller distortions in such complexes.[48]

Monocapped Clusters

There are a number of trinuclear metal clusters with only one capping ligand, classified as M_3 in Table I. These compounds have six, seven, or eight metal-core electrons and show no distortion, or insignificant distortion, from C_{3v} symmetry. A typical geometry is shown in 12.

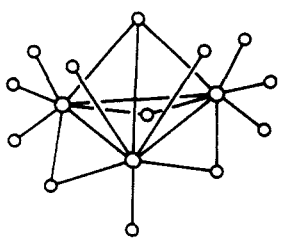

12

The adherence to threefold symmetry in the seven- and eight-electron systems is interesting. We chose as a model

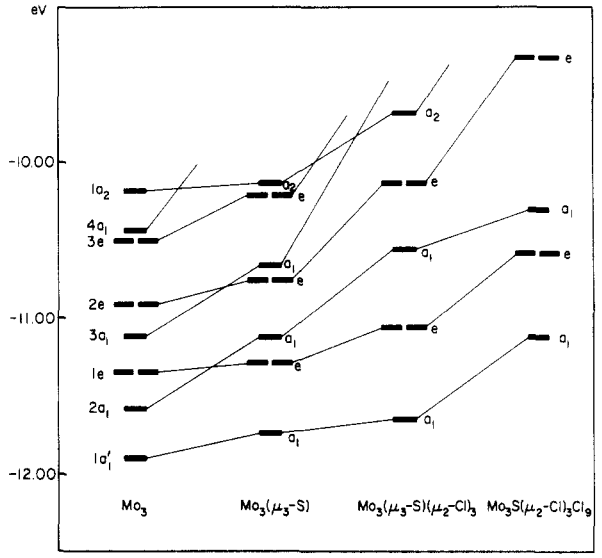

Figure 5. Evolution of the orbitals from Mo_3 to $Mo_3(\mu_3\text{-}S)$ to $Mo_3(\mu_3\text{-}S)(\mu\text{-}Cl)_3$ to $Mo_3(\mu_3\text{-}S)(\mu\text{-}Cl)_3Cl_9$.

system $Mo_3(\mu_3\text{-}S)(\mu\text{-}Cl)_3Cl_9^{2-}$ with bond lengths and angles in the $Mo_3(\mu_3\text{-}S)(\mu\text{-}Cl)_3$ core equal to those in $Mo_3S_2Cl_9^{2-}$. In the monocapped clusters the three bridging atoms move down away from the single capping ligand. The angle θ from the center of the Mo_3 triangle to a μ-Cl and the threefold axis optimizes at 60°. The terminal chlorides also adjust their position in the cluster. We next carried out a sequence of fragment calculations, just as we did in the bicapped cluster. The evolution of the orbitals from Mo_3 to $Mo_3(\mu_3\text{-}S)$ to $Mo_3(\mu_3\text{-}S)(\mu\text{-}Cl)_3$ to $Mo_3(\mu_3\text{-}S)(\mu\text{-}Cl)_3Cl_9$ is shown in Figure 5.

There is now no crossing of levels between Mo_3S and Mo_3SCl_3 and between Mo_3SCl_3 and Mo_3SCl_{12}. This is a consequence of the lower symmetry and most importantly the different geometrical location of μ-Cl atoms. In the bicapped trimers these bridging chlorides pushed $2a'_1$ way up. In the monocapped trimers the same orbital is less destabilized.

The important consequence is that the monocapped trinuclear clusters $M_3XY_3Z_6$ should be undistorted low-spin complexes for 6, 8, and 12 electrons. This is in agreement with the known experimental results. For electron counts greater than 8, but less than 12, a Jahn–Teller distortion should be observed.

Other Trimers

In recent years, Bino, Cotton, Dori, and co-workers have synthesized a number of bicapped clusters mostly with O caps, three terminal ligands, and six bridging acetate units. There is an inherent ambiguity in the way these bridges can be considered, for is an acetate a single μ ligand (13) or the equivalent of two terminal ligands (14)? Either

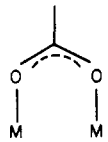

13

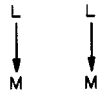

14

view could be defended, and either will produce a level sequence similar to that of $Mo_3S_2Cl_9^{3-}$, but the nature of some of the frontier MO's is quite dependent on the model used. This means we must not ignore the specific nature of each bidentate ligand if we are to deduce reliable con-

Table IV. Calculated Orbital Populations of Three Occupied Frontier Orbitals in Two Complexes

	$Mo_3(\mu_3\text{-}O)_2(O_2CH)_6(H_2O)_3$		$Mo_3(\mu_3\text{-}S)_2Cl_9^{3-}$		total no. of electrons
MO	$Mo_3O_2(H_2O)_3^{6+}$ fragment	$(O_2CH)_6^{6-}$ fragment	$Mo_3S_2^{6+}$ fragment	Cl_9^{9-} fragment	
e′	3.807	0.193	3.876	0.124	4
a'_1	1.393	0.607	1.897	0.103	2
e″	0.180	1.820	1.896	0.104	2

Table V. Bond Lengths (Å) of $[Mo_3S_2Cl_9]^{3-}$ [32]

	Mo-Mo	Mo-S	Mo-(μ-Cl)	Mo-Cl
exptl data	2.641, 2.653	2.333, 2.318	2.461, 2.468	2.442, 2.436
	2.556	2.428, 2.392	2.468, 2.456	2.437, 2.474
		2.389, 2.388	2.469, 2.481	2.429, 2.466
av (D_{2h})	2.617	2.375	2.467	2.447
av (C_{2v})	2.647, 2.556	2.326, 2.399		

Table VI. Extended Hückel Parameters

	Mo									
	H_{ij}		ζ_1		ζ_2	C_1		C_2		
5s	−8.34		1.96							
5p	−5.24		1.90							
4d	−10.50		4.54		1.901	0.590		0.590		
	S		Cl			O			H	
	H_{ij}	ζ	H_{ij}	ζ		H_{ij}	ζ		H_{ij}	ζ
3s	−20.0	1.817	−30.0	2.033	2s	−32.3	2.275	1s	−13.6	1.3
3p	−13.3	1.817	−15.0	2.033	2p	−14.8				

clusions. A calculation has been performed on the model molecule $Mo_3(\mu_3\text{-}O)_2(O_2CH)_6(H_2O)_3$ (**15**) and its various

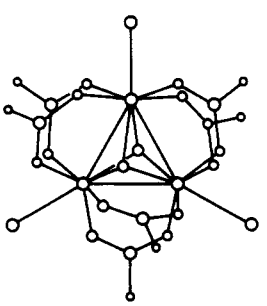

15

fragments. Bond lengths and bond angles are averaged from the experimental data, and D_{3h} molecular symmetry is assumed. Figure 6 shows the energy levels of Mo_3, $Mo_3(\mu_3\text{-}O)_2$, $Mo_3(\mu_3\text{-}O)_2(H_2O)_3$ and the complete $Mo_3(\mu_3\text{-}O)_2(O_2CH)_6(H_2O)_3$ model.

In $Mo_3(\mu_3\text{-}O)_2$ eight electrons would half-fill a degenerate level. This is different from $Mo_3(\mu_3\text{-}S)_2$, indicating the stronger ligand field of the capping oxides. When the formates are attached, one obtains in the end roughly the same level scheme as for $Mo_3S_2Cl_9$: three low-lying levels and above them a degenerate level of e″ symmetry. For a seven- or eight-electron system one might then expect a high-spin triplet or a Jahn–Teller distortion. No such complexes are as yet known with carboxylate brides. When they are made the structures will be interesting, for there is a difference between the carboxylate and chloride bridges.

In order to have an effective Jahn–Teller deformation, it is essential to have not only a part filled degenerate orbital, but the orbital must have substantial density in the region affected by a potential deformation. Otherwise the vibrational mode that is coupled will produce a splitting of the degenerate level, but the splitting will be small, ineffective in stabilization.

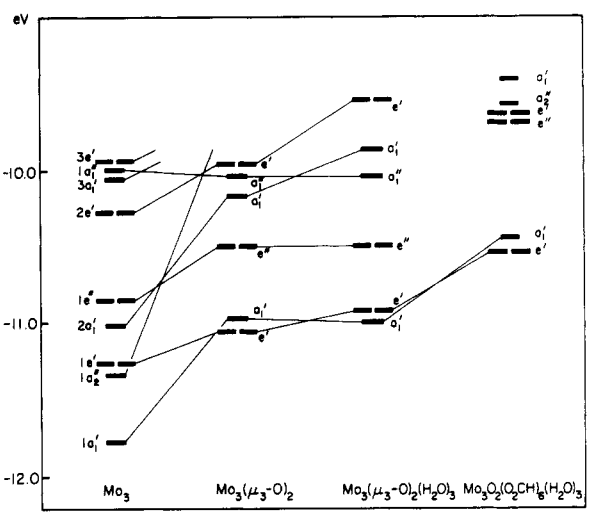

Figure 6. Correlation of frontier levels of various clusters in the construction of $Mo_3O_2(O_2CH)_6(H_2O)_3$.

In $Mo_3S_2Cl_9^{3-}$ the e″ orbital is in the Mo_3S_2 core, but in the formate it turns out to be localized on the ligands. This is shown in Table IV, which shows the electron distribution in the occupied frontier orbitals. Note the similar composition of e′ and a'_1 in the two molecules, but the very different nature of e″. In the formate e″ is primarily on the ligands. We would anticipate no "power" to distort the core but perhaps asymmetrical deformations in the carboxylate ligands.

Clusters in Molecules

In analyzing how the energy sequence of a trinuclear metallic cluster is changed by the presence of various ligand assemblies, we utilized essentially an angular overlap model argument. Also, what we did can be thought of as a generalization of the traditional ligand field theory applied to mononuclear transition-metal complexes. Similar arguments, called "cluster in molecules", have been em-

ployed by Bursten, Cotton, Hall, and co-workers. In their preceding published work dealing with trinuclear metallic clusters,[46-49] they emphasized the investigation of how the Mulliken population of the canonical valence orbitals of the metallic cluster varied with different ligand environments and analyzed the possible trend of metal-metal bond lengths. Many of our conclusions are similar. For instance, we have both deduced that the role of the terminal ligands is less important. Our study complements that of Bursten, Cotton, Hall, et al. These simplified models must be used with care. For instance, when each bidentate ligand is replaced by two terminal ligands, some frontier MO's, predominantly of ligand character, are automatically eliminated. Some fragment MO's that in the carboxylate were in the frontier MO region here are missing.

Acknowledgment. This work is an outcome of a joint USA-PRC research program supported by NSF Grant INT-8117267 and the Academia Sinica. Collaborating in this project are the groups of Lu Jiaxi, Tang Aoqing, James A. Ibers, and Roald Hoffmann. We are most grateful to F. A. Cotton, Z. Dori, and T. A. Albright for important comments, correcting some errors in an earlier version of this work.

Appendix

The experimental and idealized model geometrical parameters of $Mo_3S_2Cl_9^{3-}$ are listed in Table V.

Our calculations used the extended Hückel method,[53] with weighted H_{ij}'s.[54] The Coulomb integrals and wave functions are specified in Table VI.[55]

Registry No. 2, 92844-13-8.

(53) Hoffmann, R. *J. Chem. Phys.* **1963**, *39*, 1397.
(54) (a) Ammeter, J. H.; Bürgi, H.-B.; Thibeault, J. C.; Hoffmann, R. *J. Am. Chem. Soc.* **1978**, *100*, 3686. (b) Hoffmann, R.; Hoffmann, P. *Ibid.* **1976**, *98*, 598.
(55) Summerville, R. H.; Hoffmann, R. *J. Am. Chem. Soc.* **1976**, *98*, 7240.

Mechanisms of the Carbon–Hydrogen Bond-Forming Binuclear Reductive Elimination Reactions of Benzyl- and Hydridomanganese Carbonyls†

Mario J. Nappa, Roberto Santi, and Jack Halpern*

Department of Chemistry, The University of Chicago, Chicago, Illinois 60637

Received July 19, 1984

The reactions between $RMn(CO)_4L$ [R = *p*-$MeOC_6H_4CH_2$; L = CO (**1a**), L = (*p*-$MeOC_6H_4)_3P$ (**1c**)] and $HMn(CO)_4L$ [L = CO (**2a**), L = (*p*-$CH_3OC_6H_4)_3P$ (**2c**)] exhibit diverse stoichiometries and mechanistic pathways, depending upon the solvent and CO concentration and on whether L = CO or (*p*-$CH_3OC_6H_4)_3P$. The following reactivity patterns were identified: (1) In benzene: **1a** $\rightleftarrows$ $RMn(CO)_4$ + CO, followed by $RMn(CO)_4$ + **2a** $\rightarrow$ RH. (2) In acetonitrile or acetone (S): **1a** $\rightleftarrows$ $RCOMn(CO)_4(S)$, followed by $RCOMn(CO)_4(S)$ + **2a** $\rightarrow$ RCHO. (3) In benzene: **1c** $\rightarrow$ R· + ·$Mn(CO)_4P$, followed by R· + **2c** $\rightarrow$ RH. (4) In benzene: **1c** + CO $\rightarrow$ $RCOMn(CO)_4P$, followed by $RCOMn(CO)_4P$ + **2c** $\rightarrow$ RCHO. The kinetics of the reactions are described and the factors influencing the choice of reaction pathway discussed.

Binuclear reductive elimination reactions between transition-metal alkyls and transition-metal hydrides constitute important steps in a variety of stoichiometric and catalytic processes, for example, the product-forming steps in certain hydrogenation and hydroformylation reactions. However, only recently have such reactions received direct attention.[1] Several studies have revealed diverse reactivity patterns and led to disparate mechanistic conclusions; only in a few cases has an actual binuclear reductive elimination step been directly identified. Norton[1a] has reported that the thermal decomposition of $OsH(CH_3)(CO)_4$ is an intermolecular process and suggested that methane is formed by reductive elimination from a binuclear acyl hydride intermediate. He also reported similar reactivity patterns for reactions of iridium and rhodium acyls with osmium hydrides. More commonly, reductive elimination reactions between metal acyl and metal hydride complexes yield aldehydes. Recently, it has been suggested that the aldehyde-producing step in hydroformylation involves such a binuclear reductive elimination reaction between $RCOCo(CO)_4$ and $HCo(CO)_4$.[2] Inhibition of the reaction by CO suggests that this step involves a vacant coordination site.[3] Bergman[4] has reported that reaction between a molybdenum alkyl $CpMo(CH_3)(CO)_3$ and the corresponding hydride $CpMoH(CO)_3$ produces acetaldehyde through binuclear reductive elimination, following alkyl migration to generate a coordinatively unsaturated acyl complex. For the corresponding benzylmolybdenum complex, Mo–C bond homolysis apparently is competitive with alkyl migration and mixtures of aldehyde and toluene are formed.[4] Gladysz[5] has reported that $C_6H_5Mn(CO)_5$ reacts rapidly with

† Dedicated to the memory of Earl L. Muetterties.

(1) For recent reviews see: (a) Norton, J. R. *Acc. Chem. Res.* **1979**, *12*, 139. (b) Bergman, R. G. *Acc. Chem. Res.* **1980**, *13*, 113. (c) Halpern, J. *Inorg. Chim. Acta* **1982**, *62*, 31.
(2) Alemdaraglu, N. H.; Penninger, J. C. M.; Otlay, E. *Monatsh. Chem.* **1976**, *107*, 1153.
(3) Heck, R. F.; Breslow, D. S. *Chem. Ind. (London)* **1960**, 467. Heck, R. F. *Adv. Organomet. Chem.* **1966**, *4*, 243. Heck, R. F. "Organotransition Metal Chemistry"; Academic Press: New York, 1975; p 217.
(4) Jones, W. D.; Bergman, R. G. *J. Am. Chem. Soc.* **1979**, *101*, 5447.
(5) Tam, W.; Wong, W.-K.; Gladysz, J. A. *J. Am. Chem. Soc.* **1979**, *101*, 1589.

0276-7333/85/2304-0034$01.50/0 © 1985 American Chemical Society